Spatio-temporal mapping of ablated species in ultrafast laser-produced graphite plasmas

K. F. Al-Shboul,[a] S. S. Harilal, and A. Hassanein
Center for Materials Under Extreme Environment, School of Nuclear Engineering, Purdue University, West Lafayette, Indiana 47907, USA

(Received 13 April 2012; accepted 14 May 2012; published online 30 May 2012)

We studied the spatial and temporal distributions of ionic, neutral, and molecular species generated by femtosecond laser produced plasma under varying ambient nitrogen gas pressures. Plasmas were generated by irradiating planar graphite targets using 40 fs pulses of 800 nm radiation from a Ti:Sapphire laser. The results show that in the presence of an ambient gas, the molecular species spatial extension and lifetime are directly correlated to the evolution of excited ions. The present studies also provide valuable insights into the evolution history of various species and their excitation during ultrafast laser ablation. © *2012 American Institute of Physics*. [http://dx.doi.org/10.1063/1.4722939]

Recent experiments[1,2] showed that ultrafast lasers provide precise micromachining,[3] better laser induced breakdown spectroscopy (LIBS) signal with reduced background emission,[4] laser-ablation inductively coupled-plasma mass-spectrometry (LA-ICP-MS) with less elemental fractionation,[5] pulsed laser deposition (PLD) with less droplets,[6] etc. The generation of nanoparticles at late times during ultrafast laser plume evolution indicates that the plasma contains both non-thermal (fast) and thermal (slow) regimes.[7] In ultrafast laser-ablation (LA), the pulse duration is so short that the irradiated atoms cannot leave their lattice positions before pulse termination. This very large deposited intensity can heat up the material beyond the liquid/solid thermodynamic stability limit that can lead to nanoparticles generation.[8] In spite of several emerging applications of ultrafast LA, the fundamental understanding of the evolution of ultrafast laser produced plasmas (LPP) is still lacking. In particular, detailed investigations are needed to explore the plasma expansion dynamics and the generated excited species populations, emission, and kinetics.

In recent years, graphite based nanomaterials (graphene, diamond-like carbon, carbon nanotubes and nanowires) have become a focus for numerous studies because of their key importance both in nanoscience and nanotechnology.[9–11] Ultrafast LA of graphite can generate many of these carbon species. In this context, it was reported that carbon dimers have an essential role in the formation of these clusters and nanoparticles by chaining C_2 into higher structures.[11,12] It should be noted that the highly dynamic behavior of the LPP both in space and time and its interaction with the ambient gas strongly affect the viability and quality of these nanostructures. While much effort has been expended to characterize graphite ns LPP,[13–16] studies on spatial and temporal evolution of the emitting species in graphite fs LPP is scarce. Recent measurements performed over ns graphite LPP interaction with ambient He and N_2 showed a fairly complicated gas dynamic picture of plume-ambient gas interaction which was characterized by different propagation phases and was accompanied by intensity oscillations of various species in the plume. The presence of ambient gas was found to enhance the molecular species formation which was almost absent and limited to shorter distances and earliest times in vacuum conditions.[13,14,16,17] Optical emission spectroscopy (OES) and filtered fast imaging provide the dynamics of various emitting species during highly transient LPP expansion.[6,18] In this letter, we use a combination of these techniques to report a comprehensive picture of ionic, atomic, and molecular species evolution in femtosecond laser generated graphite plasma.

The experimental setup used in the present study is similar to the one described elsewhere.[14] The fs laser used to generate the plasma consists of a mode-locked Ti-Sapphire oscillator, stretcher, regenerative amplifier, multi-pass amplifier, and a compressor giving 10 Hz, 800 nm, 40 fs p-polarized pulses. A graphite disc was mounted inside a vacuum chamber pumped down to base pressure of about 10^{-6} Torr and then filled with nitrogen gas at a specific pressure level. An x-y-z translator was used to provide a fresh surface for each laser shot. Using a Plano-convex lens, the laser beam was focused normal to the target surface with $\sim$100 μm spot size and $\sim$87.5 J cm^{-2} fluence. An intensified charged coupled device (ICCD) was used for getting time-resolved images of the expanding plume. This 2D plume imaging was accomplished by positioning the ICCD perpendicular to the plasma expansion direction. In order to locate C_2 and CN emission zones and monitor their evolution in the plasma plume, band-pass filters were used for filtering C_2 Swan band (0-0) transition at 516.5 nm and CN Violet (0-0) transition at 388.3 nm. A 0.5 m spectrograph in conjunction with a 2 ns rise time photomultiplier tube (PMT) was used for performing time and space resolved emission spectroscopy. Using this setup a time-of-flight profile for each excited species under investigation was generated with very high spectral purity in addition to very high time resolution.

To understand the mechanisms behind the molecular formation during ultrafast LA of graphite, ambient nitrogen (at various pressures) was used to generate reactive species like CN along with carbon dimers (C_2). Though CN is formed purely due to recombination, the generation of carbon dimers in LPP can be due to several formation mechanisms including recombination, dissociation of higher carbon clusters, and ejection directly from the target

[a]Electronic mail: kalshbou@purdue.edu.

surface.[15] Typical spectrally integrated (350–700 nm) images along with monochromatic images of C_2 and CN for the fs graphite LPP are given in Fig. 1. The gating time of these images is incrementally increased (2–100 ns) to compensate for the reduction in plasma intensity at later times. Comparing the images shows that the spectrally integrated emission distribution appears broader because of sampling of all the excited species in the plasma emitting in the visible range traveling with different velocities. Emission from both C_2 and CN is more evident at later stages of the plasma expansion especially at the plasma peripheries due to enhanced recombination probability at the plume-gas interface zones.[17]

In contrast to the spherical-like ns LPPs[13,14,17] where plume intensity oscillations were evident, Fig. 1 shows the forward-centric expansion features of fs LPP plume that can be best represented by a unimodal distribution. In ultrashort LA the electron to ion energy transfer time (τ_{ei}) and heat conduction time (t_{heat}) exceeds the duration of the excitation laser pulse ($\tau_{ei} \sim t_{heat} \gg t_p$). Hence the laser light is absorbed most efficiently by the target surface in the laser impact zone and the plasma formation takes place after the end of the laser pulse. Thus, the preferential expansion of fs plasma along the target normal can be understood by considering the high plasma pressure at initial time due to the strong overheating. During fs LA, CN bright emission was noticed only at the plume fronts and wings. On the other hand, a bright C_2 emission zone was visible near the target (<1 mm) at early times. This emission peak is also noticed in vacuum, (not shown in Fig. 1) where the location of the C_2 emission is constrained at short distances and very early times. It should be noted that for ablation in vacuum, the collisional processes predominantly occur near the target at the earliest times where the density is highest. So the origin of the emission zone near the target surface could be due to direct ablation from the target or formed through three-body collisions. Similar phenomena have been reported previously for ns laser-generated graphite plasmas.[16]

With evolving time, C_2 emission becomes brighter in the wings rather than in the plume front especially at 1 and 5 Torr N_2. Our recent results showed that the high energetic ions emanating from ultrafast laser plasmas are confined in a small cone angle with respect to target normal.[19] Hence, dissociation of C_2 in plume front positions is highly probable considering its lower dissociation energy[20] (6.27 eV) compared to CN molecules (7.72 eV). On the other hand, the lower temperature in the plasma wings will enhance three-body recombination which is proportional to $(n_e^2.T_e^{-9/2})$ with T_e in eV and n_e in m^{-3}.[21] The ICCD images can also be used for gaining better insights of the plasma expansion dynamics and kinetics by generating position-time (R-t) plots. Typical R-t plots obtained for the plasma plume front from the spectrally integrated images at different nitrogen pressure levels are given in Fig. 2. The R-t plots show that the plasma plume expansion is well described by the drag force model.[22] This model has been used previously for describing ns LPP expansion at moderate pressures by assuming plume deceleration due to drag forces created by surrounding gas, and this deceleration is proportional to the plasma expanding velocity.[22] The estimated plume stopping distances according to this model were found to be 9, 7.1, and 4.8 mm for 0.4, 1, and 5 Torr nitrogen pressures, respectively, which are in good agreement with the experimental values obtained by the ICCD images.

ICCD spectrally filtered images of C_2 and CN provided contrasting evolutions at particular time during the plume evolution. We utilized optical time-of-flight emission-spectroscopy (OTOF-ES) experiments to get better insights of the expansion dynamics of emitting zones of various

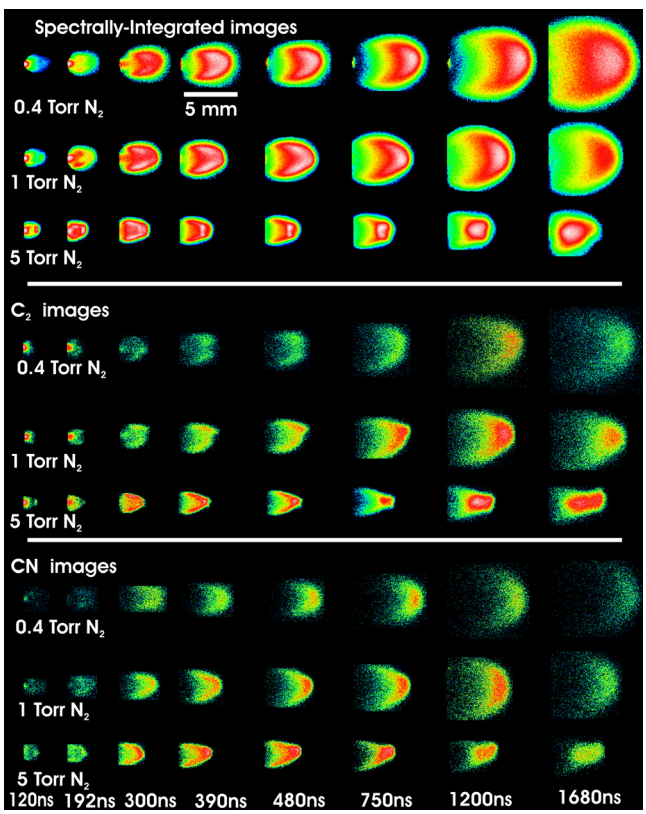

FIG. 1. Spectrally integrated, C_2, and CN monochromatic images of graphite plasma at 0.4, 1, and 5 Torr N_2 pressures. Each image is normalized to its maximum intensity for better clarity.

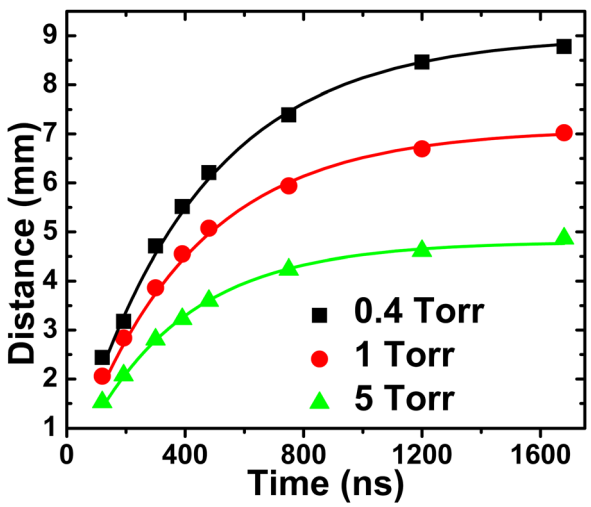

FIG. 2. Position–time (R-t) plots of the plume front at 0.4, 1, and 5 Torr nitrogen pressures measured from the spectrally integrated ICCD plume images. The symbols represent experimental data points and solid curves represent the drag expansion model.

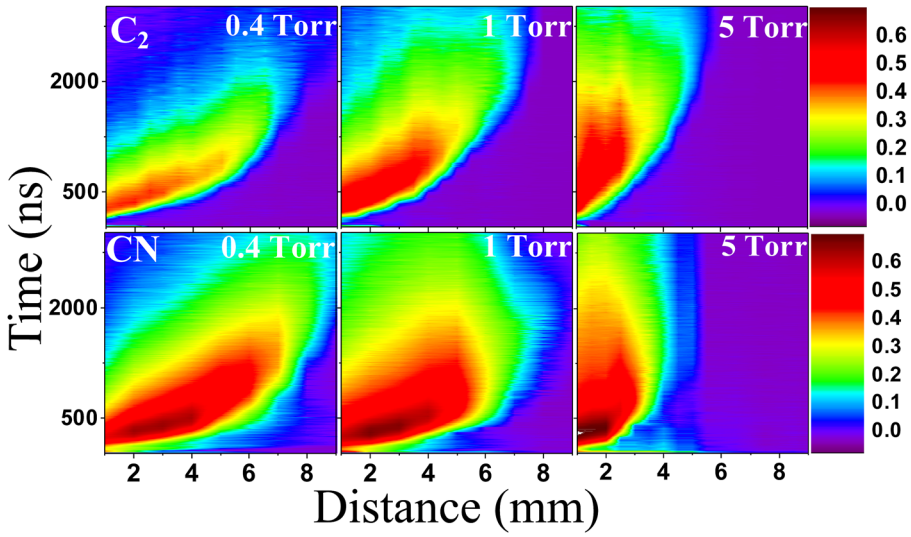

FIG. 3. Space-time contours for C_2 ($\lambda = 516.5$ nm) and CN ($\lambda = 388.3$ nm) in N_2 gas at 0.4, 1, and 5 Torr pressure levels.

excited carbon species including CN generated after the ultrafast LA of graphite. The TOF measurements were used to generate distance-time contours for various excited species and the results are presented in Fig. 3 for C_2 and CN. Both C_2 and CN contours show a broad peak emission which is expected for molecular species emission. Unlike ns LPP (Refs. 13, 14, and 17) where the molecular species showed a bimodal distribution, C_2 and CN distributions in fs LPP are more uniform and mostly formed in the plume front positions when the plasma interacts with ambient gas. This could indicate that the molecular species formation in fs plume is mainly due to recombination of higher charged ions and excited neutrals.[17] In order to confirm this hypothesis, we investigated the space-time contours of neutrals and various ionic species emitting in the visible region under similar experimental conditions. The temporal profiles and corresponding space-time contours of excited neutral carbon at 247.8 nm ($3s$; $^1P^\circ \rightarrow 2p^2$; ^1S), singly ionized carbon at 426.7 nm ($4f$; $^2F^\circ \rightarrow 3d$; ^2D), and doubly ionized carbon at 406.9 nm ($5g$; $^3G \rightarrow 4f$; $^3F^\circ$) at vacuum and various N_2 pressure levels were also recorded and are given in Fig. 4. The contours given in Fig. 4 show that in vacuum all species studied expand freely as indicated by the single peak emission distribution which is restricted to short time scales because of reduced recombination processes. With the addition of more nitrogen another delayed and more intense peak appeared for neutral as well as ionized C species. It is also interesting to note that the emission intensity from vacuum free expansion peak is getting weaker with increasing pressure and in the case of C^{2+} is totally disappeared in all ambient pressure levels studied.

Previous studies using ICCD imaging showed two shock fronts during ultrafast laser created graphite plasma expansion into ambient Ar gas[17]; the faster component was explained due to highly energetic non-thermal ejection mechanisms and the slower component was caused by thermally ejected carbon atoms and clusters. Though the present work showed similar multi-peak structure in the space-time contours, the plume splitting was evidently absent in the ICCD images. This could be because of the low photon counts and/or the dynamic range of ICCD is not high enough to expose these photons. For better details about the expansion dynamics of various component species in the plumes, R-t plots were obtained from the OTOF-ES data and are

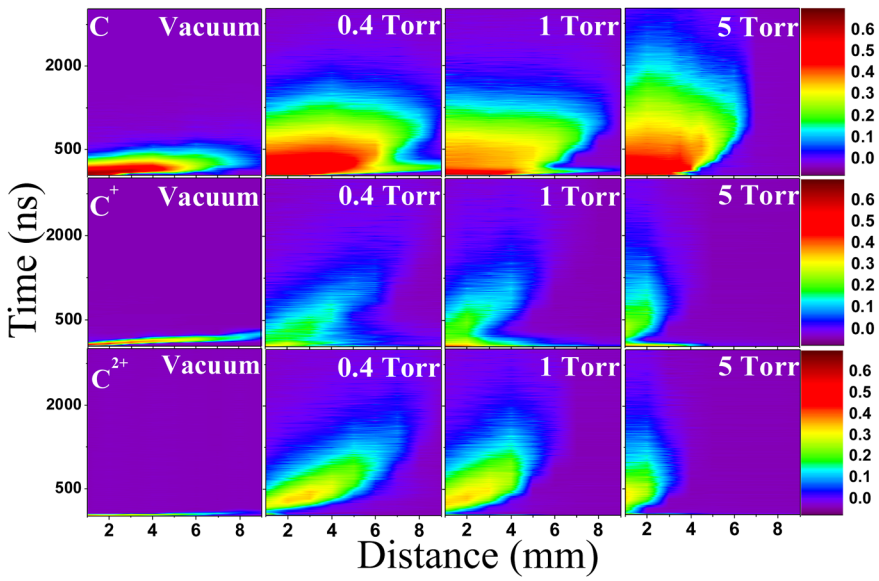

FIG. 4. Space-time contours for C ($\lambda = 247.8$ nm), C^+ ($\lambda = 426.7$ nm), and C^{2+} ($\lambda = 406.9$ nm) in vacuum and N_2 gas at 0.4, 1, and 5 Torr pressure levels.

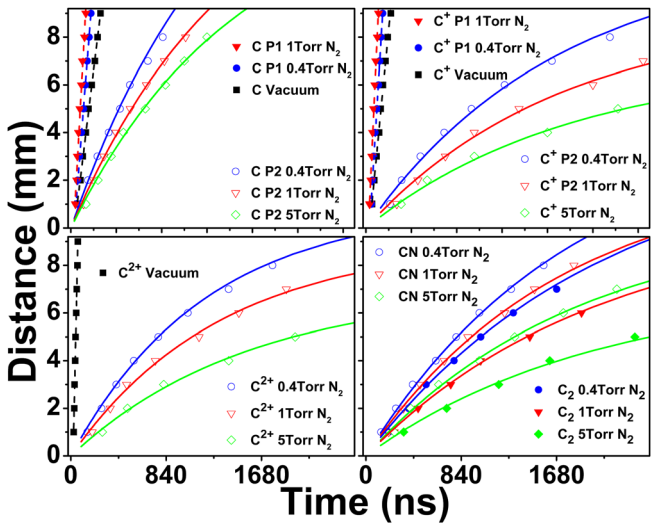

FIG. 5. Position–time (R-t) plots for CN, C_2, C, C^+, and C^{2+} in vacuum and nitrogen at various pressures measured from the corresponding space-time contours. P_1 and P_2 refer to the early and delayed peaks, respectively, for the noticed double-peak structure of C and C^+ in the presence of ambient nitrogen. The symbols represent experimental data points, dash lines represent linear fittings, and solid curves represent the drag expansion model.

given in Fig. 5. Among the species studied, C^{2+} possessed the highest kinetic energy (~2.7 keV) with a good agreement with previously reported values at similar experimental conditions.[23] The R-t plots also show that, rather surprisingly, the free expansion peaks of neutral C and C^+ species are found to be faster with increasing ambient nitrogen pressure. For example, the recorded kinetic energies of the free expanding peaks of neutral C and C^+ (straight dash line fits in Fig. 5) are 90 and 149 eV at vacuum, and their values increased to 230 and 380 eV at 0.4 Torr and 460 and 675 eV at 1 Torr, respectively. This rise in kinetic energies can be correlated to enhanced recombination of faster moving ions with increasing ambient gas pressures.[21]

Fig. 5 shows that the delayed emission peaks of neutral C species are faster compared to the delayed peaks of C^+ with increasing ambient nitrogen pressure. Similar observation was noticed during carbon plume expansion in the presence of Ar ambient and explained due to C^+ generated by impact ionization of neutral C.[17] Referring back to Fig. 3, it shows that the CN zones with the highest intensity are correlated to those of C^{2+} in Fig. 4. Moreover, Fig. 5 shows that the temporal expansion of CN is in good agreement with C^{2+} expansion. These observations indicate that the early CN formation is due to C^{2+} recombination with nitrogen gas.[24] Similarly, Figs. 3–5 show that C_2 early emission is correlated to C^+ delayed peak recombination.[13] The comparison of C_2 and CN expansion dynamics and the position of the plume front in their monochromatic images and their space-time contours indicate that at early times of plasma expansion CN and C_2 molecules are formed due to fast ions recombination and then at later stages of the plasma life, C_2 generated by slower higher carbon clusters dissociation becomes a precursor to CN formation according to the following reaction[24]: $C_2 + N_2 \rightarrow 2CN$ which explains the broad distribution of CN and C_2.

In conclusion, we investigated C_2 and CN formation dynamics in graphite fs LPP in ambient nitrogen gas using a combination of filtered fast imaging and OTOF-ES. The filtered images showed the role of the ambient gas on recombination especially at the plume-gas interface zones. The carbon plume produced by ultrafast LA in the presence of moderate ambient nitrogen pressures is well described by the drag model. The space-time contours of various species investigated in the ultrafast laser produced plume show that in the presence of an ambient gas the spatio-temporal extent of each species is related to its next ionized level and the molecular species spatial extension at the early stages of the plasma life are directly correlated to the excited ions. The present studies provide an insight into the generation and evolution of various species in ultrafast laser created graphite plumes.

The authors thank Brandon Verhoff for experimental assistance. This work was partially supported by the US DOE, office of National Nuclear Security Administration (Contract No. DE-NA0000463).

[1]H. Dachraoui and W. Husinsky, Appl. Phys. Lett. **89**, 104102 (2006).
[2]B. Liu, Z. D. Hu, Y. Che, Y. B. Chen, and X. Q. Pan, Appl. Phys. Lett. **90**, 044103 (2007).
[3]M. Q. Ye and C. P. Grigoropoulos, J. Appl. Phys. **89**, 5183 (2001).
[4]D. J. Hwang, H. Jeon, C. P. Grigoropoulos, J. Yoo, and R. E. Russo, Appl. Phys. Lett. **91**, 251118 (2007).
[5]R. E. Russo, X. L. Mao, J. J. Gonzalez, and S. S. Mao, J. Anal. At. Spectrom. **17**, 1072 (2002).
[6]O. Albert, S. Roger, Y. Glinec, J. C. Loulergue, J. Etchepare, C. Boulmer-Leborgne, J. Perriere, and E. Millon, Appl. Phys. A - Mater. Sci. Process. **76**, 319 (2003).
[7]S. Amoruso, R. Bruzzese, X. Wang, and J. Xia, Appl. Phys. Lett. **92**, 041503 (2008).
[8]S. Eliezer, N. Eliaz, E. Grossman, D. Fisher, I. Gouzman, Z. Henis, S. Pecker, Y. Horovitz, M. Fraenkel, S. Maman, and Y. Lereah, Phys. Rev. B **69**, 144119 (2004).
[9]A. C. Dillon, P. A. Parilla, J. L. Alleman, J. D. Perkins, and M. J. Heben, Chem. Phys. Lett. **316**, 13 (2000).
[10]F. Qian, R. K. Singh, S. K. Dutta, and P. P. Pronko, Appl. Phys. Lett. **67**, 3120 (1995).
[11]M. K. Moodley and N. J. Coville, Chem. Phys. Lett. **498**, 140 (2010).
[12]A. Van Orden and R. J. Saykally, Chem. Rev. **98**, 2313 (1998).
[13]K. F. Al-Shboul, S. S. Harilal, and A. Hassanein, Appl. Phys. Lett. **99**, 131506 (2011).
[14]K. F. Al-Shboul, S. S. Harilal, A. Hassanein, and M. Polek, J. Appl. Phys. **109**, 053302 (2011).
[15]Y. Iida and E. S. Yeung, Appl. Spectrosc. **48**, 945 (1994).
[16]S. Acquaviva and M. L. De Giorgi, Appl. Surf. Sci. **197–198**, 21 (2002).
[17]S. J. Henley, J. D. Carey, S. R. P. Silva, G. M. Fuge, M. N. R. Ashfold, and D. Anglos, Phys. Rev. B **72**, 205413 (2005).
[18]D. Grojo, J. Hermann, and A. Perrone, J. Appl. Phys. **97**, 063306 (2005).
[19]B. Verhoff, S. S. Harilal, and A. Hassanein, "Angular emission of ions and mass deposition from femtosecond and nanosecond laser-produced plasmas," J. Appl. Phys. (submitted).
[20]A. D. Pradhan, H. Partridge, and J. C. W. Bauschlicher, J. Chem. Phys. **101**, 3857 (1994).
[21]P. T. Rumsby and J. W. M. Paul, Plasma Phys. **16**, 247 (1974).
[22]A. K. Sharma and R. K. Thareja, Appl. Surf. Sci. **243**, 68 (2005).
[23]P. A. VanRompay, M. Nantel, and P. P. Pronko, Surf. Coat. Technol. **100**, 496 (1998).
[24]G. M. Fuge, M. N. R. Ashfold, and S. J. Henley, J. Appl. Phys. **99**, 014309 (2006).